

THE DESIGN OF A PROTON SPECTROMETER FOR 60-200 MeV ENERGY RANGE

Lucian TUDOR¹, Florin NEGOITA², Dan STUTMAN³, Calin Alexandru UR⁴,
Marius GUGIU⁵, Andi CUCOANES⁶, Cristian MANAILESCU⁷, Florin
ROTARU⁸, Stanimir KISYOV⁹

A new proton spectrometer has been designed using analytical calculations and SIMION v7, a specific software for charged particle trajectory simulations, to measure the energy distribution of protons accelerated by the high power (TW, PW) lasers interaction with solid targets. The resulting device has a high versatility due to its architecture, which uses a pinhole, one permanent magnetic core and a detection screen, being intended as magnetic section of a Thomson parabola. In the simulated configuration, proton position distribution on the detection plane is converted in energy over a range from 60 MeV to 200 MeV. Energy resolution was calculated as function of proton energy, for an angular acceptance of 1 mrad defined by pinhole.

Keywords: Proton spectrometer design

1. Introduction

¹ ELI-NP, Horia Hulubei National Institute for Physics and Nuclear Engineering, 30 Reactorului Street, 077125 Magurele, Ilfov County, Romania; University Politehnica of Bucharest, 313 Splaiul Independentei, Sector 6, 060042 Bucharest, Romania; email: lucian.tudor@eli-np.ro;

² ELI-NP, Horia Hulubei National Institute for Physics and Nuclear Engineering, 30 Reactorului Street, 077125 Magurele, Ilfov County, Romania; Horia Hulubei National Institute for Physics and Nuclear Engineering, 30 Reactorului Street, 077125 Magurele, Ilfov County, Romania;

³ ELI-NP, Horia Hulubei National Institute for Physics and Nuclear Engineering, 30 Reactorului Street, 077125 Magurele, Ilfov County, Romania;

⁴ ELI-NP, Horia Hulubei National Institute for Physics and Nuclear Engineering, 30 Reactorului Street, 077125 Magurele, Ilfov County, Romania; University Politehnica of Bucharest, 313 Splaiul Independentei, Sector 6, 060042 Bucharest, Romania;

⁵ ELI-NP, Horia Hulubei National Institute for Physics and Nuclear Engineering, 30 Reactorului Street, 077125 Magurele, Ilfov County, Romania; Horia Hulubei National Institute for Physics and Nuclear Engineering, 30 Reactorului Street, 077125 Magurele, Ilfov County, Romania;

⁶ ELI-NP, Horia Hulubei National Institute for Physics and Nuclear Engineering, 30 Reactorului Street, 077125 Magurele, Ilfov County, Romania;

⁷ Horia Hulubei National Institute for Physics and Nuclear Engineering, 30 Reactorului Street, 077125 Magurele, Ilfov County, Romania;

⁸ ELI-NP, Horia Hulubei National Institute for Physics and Nuclear Engineering, 30 Reactorului Street, 077125 Magurele, Ilfov County, Romania; Horia Hulubei National Institute for Physics and Nuclear Engineering, 30 Reactorului Street, 077125 Magurele, Ilfov County, Romania;

⁹ ELI-NP, Horia Hulubei National Institute for Physics and Nuclear Engineering, 30 Reactorului Street, 077125 Magurele, Ilfov County, Romania;

Protons acceleration driven by high-power lasers is becoming more and more interesting over the last decade, as the range of applications is broad including medicine, industry and science. Proton acceleration mechanisms, such as Radiation Pressure Acceleration (RPA) [1], Break-out Afterburner (BOA) [2] or Target Normal Sheath Acceleration (TNSA) [3] are intense subjects of research, the energy range predicted by the acceleration methods mentioned above extends well above 100 MeV, which represents roughly the maximum energy currently achieved for protons [4]. A proton spectrometer is able to measure with high resolution the energy spectra of protons accelerated in a single laser shot [5], as part of the laser-accelerated proton bunch characterization required in terms of energy, angular divergence, as well as shot-to-shot reproducibility. The proton spectrometer measure a little part of proton emission due to the low angular acceptance, but it has a large acceptance in terms of energy and is immune to electromagnetic pulses (EMP) [6], when coupled to passive detectors. In a proton spectrometer, magnetic fields are used to deflect protons that can be observed at the detector plane (see Fig.1). The proton spectrometer can be coupled to several types of detectors, which can operate in different reading regimes: for an ‘offline’ reading, radiochromic films (RCF-s), image plates (IP-s) [7] and CR39 (plastic solid state nuclear track detectors) [8] can be used. The ‘online’ reading approach uses classical scintillators or LANEX scintillator screens [9] viewed by a triggerable CCD camera. In order to amplify the signal a multichannel plate (MCP) amplifier can be used [10]. In this paper, we report a new design for a versatile proton spectrometer for the energy range of 60 – 200 MeV, together with associated performance simulations.

2. Proton spectrometer design

The structure of the device consists of a pinhole, a permanent magnetic core and a detection screen (see Figures 1 to 4). The proton beam is sent through the pinhole, which serves as a spatial filter, and propagates on the Ox axis. The proton beam at output of the pinhole enters in the 1 Tesla magnetic field B , oriented along the Oy axis, which is perpendicular on the magnetic plates. The magnetic field was obtained by implementing a magnetic core with the magnets poles having the length L and separated by a gap of width W as shown in Figure 3. The profile of the magnetic field along the propagation axis of the proton beam is uniform within a wide region in the center of the magnet (200 mm-350 mm), as shown in Figure 2. While inside the magnetic field, the charged particles have their trajectories curved under the action of the Lorentz force, and depending on the velocity of the protons, a spatial distribution can be observed on a detection screen placed at a distance DL from the output of the magnetic core (see Figure 1). This architecture, together with the magnetic field design ensures that the proton spectrometer can be used to detect protons with energies ranging from 60 to 200 MeV when detection positions span not more than 5 cm distance convenient to be viewed with a CCD camera.

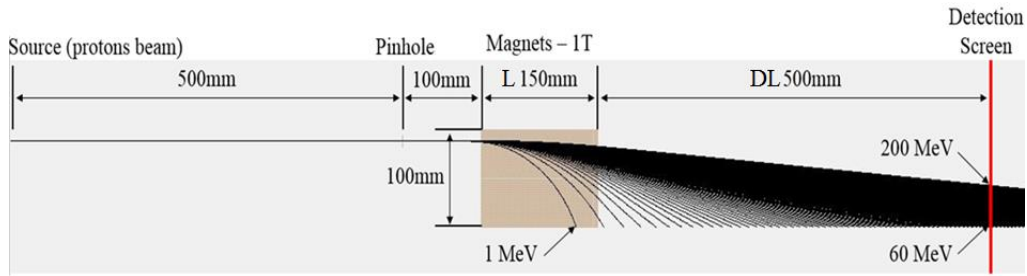


Fig.1. Side view of the Proton Spectrometer placed along the beam initial propagation direction.

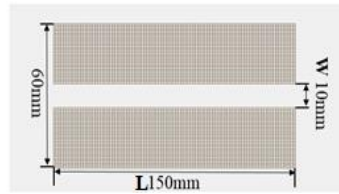
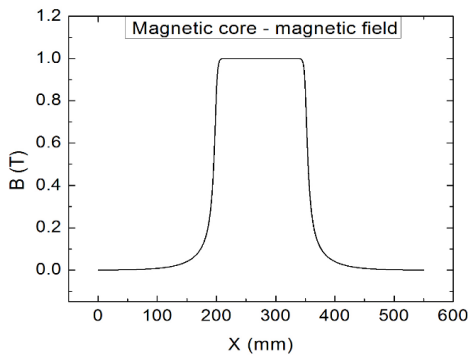


Fig. 3. Magnetic core

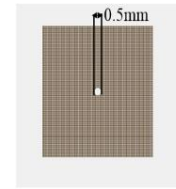


Fig. 4. Pinhole

Fig. 2. Magnetic field profile along the propagation axis

3. SIMION simulations and analytical calculations

The determination of the proton trajectories was done using two methods: first we used SIMION v7, a specific software for charged particle trajectory simulations in electromagnetic fields and second, we performed analytical calculations based on the geometry of the device and magnetic field values. The analytical calculations were done under the assumption that the protons have both relativistic and, respectively non-relativistic (classical) kinematics.

3.1. Non-relativistic (classical) proton deflection

In the classical case, the coordinate of the deflected proton is given by [11]:

$$x_m = \frac{q \cdot B \cdot L}{\sqrt{2 \cdot m \cdot KE}} \left(DL + \frac{L}{2} \right) \quad (1)$$

where q is the charge of the proton, B is the average value of the magnetic field, m is the mass, KE is the kinetic energy, L is the length of the magnetic field and DL is the distance from the exit of the magnetic field to the detector plane. Under the design considerations shown in the Figure 1, the obtained results for the deflection are plotted in the Fig. 5.

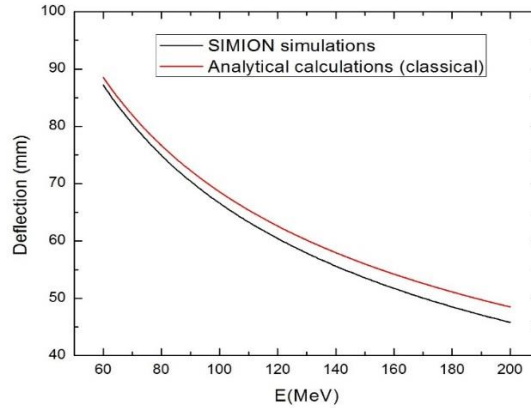


Fig. 5. Proton deflection in the detection plane after pasage through the magnetic field with, $B_{max}=1T$, SIMION simulations are plotted with black line and analytical calculations (classical case) with red line.

In the two simulations depicted in the Figure 5, the deviation of the analytical curve with respect to the SIMION curve increases with energy, ranging from 1.49% at 60MeV to 5.89% at 200 MeV. In order to achieve a better overlap between the two curves, the relativistic motion must be taken into account.

3.2. Relativistic proton deflection

For the relativistic case, all geometric and field considerations involved in the construction of the spectrometer remain the same as in the classical case. In both cases, the Lorentz force acts as a centripetal force:

$$F_{cp} = F_L \Leftrightarrow \frac{mv^2}{R} = evB \Rightarrow R = \frac{mv}{eB} \quad (2)$$

but, in the relativistic case, the mass of the proton varies with its velocity $m = \gamma m_0$, where γ represents the Lorentz factor:

$$\gamma = \frac{1}{\sqrt{1 - \frac{v^2}{c^2}}} \quad (3)$$

and therefore R^2 becomes:

$$R^2 = \frac{m^2 v^2}{e^2 B^2} = \frac{m^2 c^2 \left(1 - \frac{1}{\gamma^2}\right)}{e^2 B^2} \quad (4)$$

With the curvature radius determined, the deflection Δ can be calculated according to the geometrical model presented in the Fig. 6.

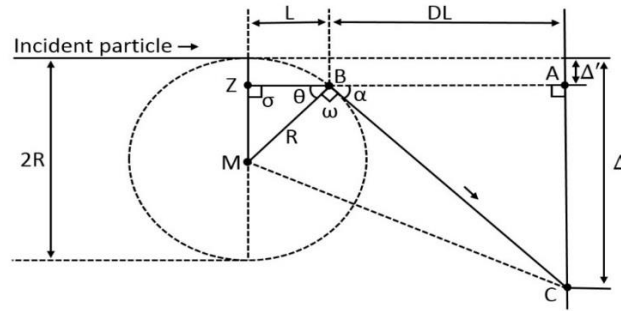


Fig. 6. Geometrical model

$$\text{In } \triangle MBZ, \sphericalangle \sigma = 90^\circ \Rightarrow MZ = \sqrt{MB^2 - ZB^2}, MB = R, ZB = L \quad (5)$$

$$R = MZ + \Delta' \Rightarrow \Delta' = R - MZ \quad (6)$$

$$\sphericalangle \theta = \arcsin \frac{MZ}{MB}, \text{ in } \triangle MBC \sphericalangle \omega = 90^\circ \Rightarrow \sphericalangle \alpha = 180^\circ - 90^\circ - \sphericalangle \theta \quad (7)$$

$$\text{In } \triangle ABC \quad \text{tg } \alpha = \frac{\Delta - \Delta'}{DL} \Rightarrow \Delta = DL \cdot \text{tg } \alpha + \Delta' \quad (8)$$

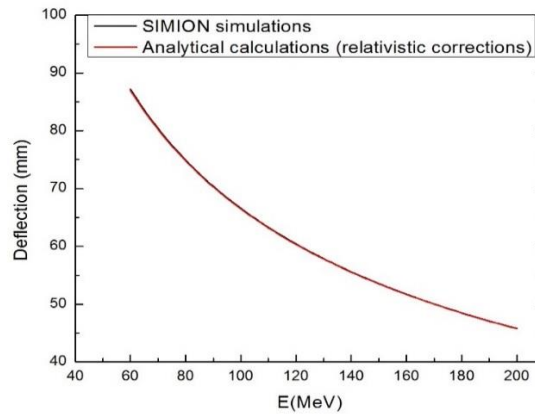


Fig. 7. Proton deflection in the detection plane after passage through the magnetic field with, $B_{\max}=1\text{T}$., SIMION simulations are plotted with black line and analytical calculations (relativistic case) with red line.

The formulas describing the model have been implemented into a computer code. The input variables for the program were: the proton energy, the average value of the magnetic field B , the length of the magnetic field L , the distance from the exit of the magnetic field to the detector plane DL , and the outputs were the radius of curvature R , deflection in the magnetic field Δ' , exit angle from the magnetic field region α , and total deflection Δ . The obtained simulation results are presented in the Fig. 7. The relativistic calculations offer a relative difference to the

SIMION simulation curve of 0.31% at 60 MeV and 0.1% at 200 MeV, increasing the accuracy of the analytical calculations by at least one order of magnitude when compared to the results obtained in the classical case. The results regarding accuracy are presented in Fig. 8.

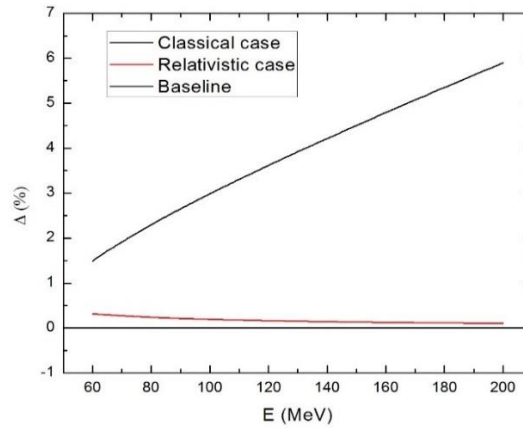


Fig. 8. The relative difference between SIMION simulation (baseline) and the analytical calculations, classical case and relativistic case, for protons with energies between 60 to 200 MeV.

4. Proton spectrometer resolution

A key feature of the proton spectrometer is the resolution. This parameter is defined as the square root of the variance of the spectrometer energy distribution response for incoming monoenergetic protons. To determine the resolution a conical proton beam, spatially filtered by a 0.5 mm pinhole was used (see Fig. 9). The pinhole was placed along the beam, in the geometry described in the Fig. 1. The spatial distribution of the 100 MeV proton beam after it has passed through the pinhole and spectrometer can be observed in Fig. 10. This deflection distribution can be converted to an energy distribution based on the position calibration and the curve described above, allowing to extract the energy resolution at the given proton beam energy.

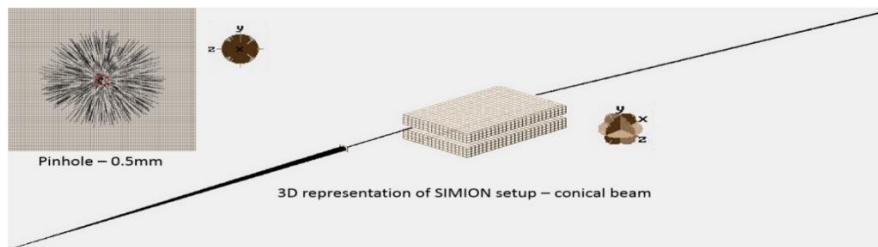


Fig. 9. 3D representation of SIMION setup using a conical beam.

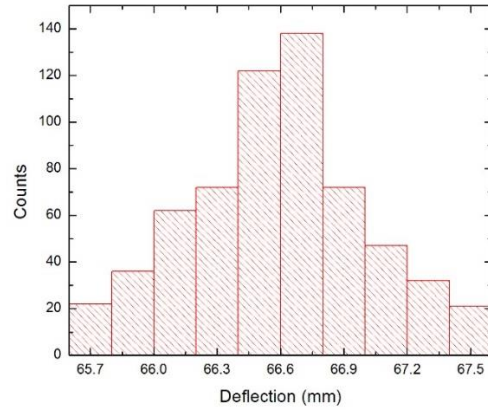


Fig. 10. The spatial distribution histogram for 100 MeV proton beam.

Thus, using the chosen proton spectrometer configuration we have achieved a resolution ranging from 0.5 MeV for protons with 60 MeV energy up to 3.7 MeV for protons with 200 MeV energy, as depicted in the Fig. 11.

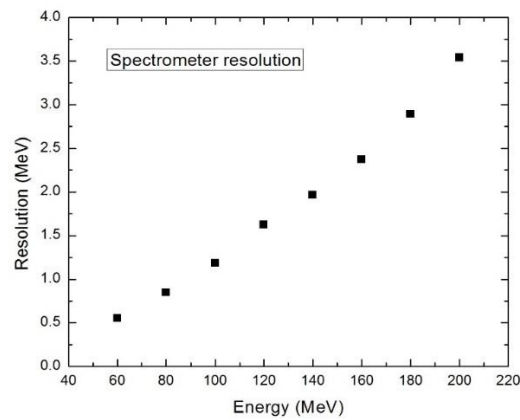


Fig. 11. The proton spectrometer resolution for protons with energies between 60 to 200 MeV.

The resolution is obviously improved when the angular acceptance, defined by the pinhole diameter and its distance to source point, is decreased. The minimum acceptance to be used when measurements are performed will be actually determined by the sensitivity of the detectors used for position readout and the measured proton yields.

5. Conclusions

We report a new design for a proton spectrometer, with the capability to measure protons with good energy resolution in the 60 - 200 MeV energy range. For 1 mrad angular acceptance the energy resolution varies between 0.5 MeV (at 60 MeV of protons) and 3.7 MeV (at 200 MeV of protons). The SIMION simulations have been successfully compared with analytical calculations, the relative difference between simulations made with SIMION and the analytical calculations being only 0.31% in the best approximation, under relativistic kinematics.

REFERENCES

- [1]. *A.P.L. Robinson et al*, "Radiation pressure acceleration of thin foils with circularly polarized laser pulses", *New Journal of Physics*, January, **10**, 2008.
- [2]. *L. Yin et al*, "Monoenergetic and GeV ion acceleration from the laser breakout afterburner using ultrathin targets", *Physics of Plasmas*, April, **14**, 2007.
- [3]. *S. C. Wilks et al*, "Energetic proton generation in ultra-intense laser–solid interactions", *Physics of Plasmas*, February, **8**, 2001.
- [4]. *F. Wagner et al*, "Maximum Proton Energy above 85 MeV from the Relativistic Interaction of Laser Pulses with Micrometer Thick CH₂ Targets", *Phys. Rev. Lett.*, May, **116**, 2017.
- [5]. *Daniel Jung*, "Ion acceleration from relativistic laser nano-target interaction", Dissertation an der Fakultät für Physik der Ludwig Maximilians Universität München, Munchen, January, 2012.
- [6]. *M. Mead et al*, "Electromagnetic pulse generation within a petawatt laser target chamber", *Review of Scientific Instruments*, October, **75**, 2004.
- [7]. *A. Mančić et al*, "Absolute calibration of photostimulable image plate detectors used as (0.5-20 MeV) high- energy proton detectors", *Review of Scientific Instruments*, July, **79**, 2008.
- [8]. *D.C. Carrolla et al*, "A modied Thomson parabola spectrometer for high resolution multi-MeV ion measurements - application to laser-driven ion acceleration", *Nuclear Instruments and Methods in Physics Research Section A*, November, 2009.
- [9]. *B. Hidding et al*, "Study of Space Radiation Effects with Laser-Plasma-Accelerators", ESA NPI Activity, Final Report, Hamburg, Germany, 2013.
- [10]. *M. Cutroneo et al*, "Thomson parabola spectrometry of laser generated plasma at PALS laboratory", *Journal of Physics Conference Series* 508, April, 2014.
- [11]. *C. G. Freeman et al*, "Calibration of a Thomson parabola ion spectrometer and Fujifilm imaging plate detectors for protons, deuterons, and alpha particles", *Review of Scientific Instruments*, July, **82**, 2011.